In vitro and *in vivo* cytotoxic effect of AntiGan against tumor cells

VALTER R.M. LOMBARDI[1], IVÁN CARRERA[1] and RAMÓN CACABELOS[2]

[1]Department of Health Biotechnology, EuroEspes Biotechnology; [2]EuroEspes Biomedical Research Center, Institute for CNS Disorders and Genomic Medicine, 15165 Corunna, Spain

Abstract. Novel effective chemopreventive agents against cancer are required to improve current therapeutic rates. The aim of the present study was to investigate the anti-carcinogenesis effect of AntiGan, an extract obtained from the European conger eel, *Conger conger, in vitro* (human tumor cell lines) and *in vivo* (murine model of colitis) models. The potential apoptogenic activity after 24 h of incubation with 10, 25 and 50 μl/ml AntiGan was reported using growth inhibition and apoptosis activity assays. *In vivo* studies were performed in mice by inducing colitis with oral administration of 2% dextran sulphate sodium (DSS) for 5 weeks. Apoptosis was observed in HL-60, Hs 313.T, SW-480, Caco-2 and HT-29 cell lines. The highest level of growth inhibition was observed in Caco-2 (66, 75.8 and 88.1%), HT-29 (56, 73 and 87.6%) and SW-480 (38.5, 61.6, 78.6%) for AntiGan doses of 10, 25 and 50 μl/ml, respectively, compared to untreated cells, while the results of the expression of genes associated with apoptosis indicated a downregulation of B-cell lymphoma 2 (Bcl-2) in all cell lines studied. *In vivo*, morphopathological alterations in the colon were analyzed by immunohistochemical and staining methods. Tumoral markers, including β-catenin, cyclooxygenase 2 and Bcl-2 were expressed in cryptal cells of the dysplastic colonic mucosa, whereas the levels of interferon-γ expression were also increased when no treatment was applied. In the experimental murine model, the optimal concentration of AntiGan for an effective dose-response was 10% in diet. These results suggested that AntiGan displays a powerful anti-inflammatory effect in DSS-induced colitis, acting as a chemopreventive agent against colon carcinogenesis, most likely due to its apoptogenic peptides that contribute to the induction of apoptosis.

Introduction

Major advances in the management of cancer have been achieved since cancer chemotherapy, as we know it today, began to take shape with the discovery of the antitumoral activity of alkylating agents (1), certain hormones (2) and the advent of antimetabolites of DNA building blocks (3). In addition, aberrant histone methylation associated with gene mutation, translocation or overexpression may often lead to initiation of a disease process leading to cancer (3,4). In recent years, some specific molecule inhibitors of such histone modifying enzymes that correct their abnormal methylation are being used as novel therapeutics for these pathologies (4). In the 1960s a clinical study investigating combination therapy, brought about major advances, leading to the demonstration that complete remission of certain neoplasia could be induced with available anticancer drugs (5). At the same time, novel agents, including anthracycline antibiotics, the *Vinca* alkaloids, the platinum complexes and hormone antagonists, provided additional powerful tools (5-7). The advances in cancer chemotherapy were also greatly aided by progress made in diagnostic procedures, by the advent of combined modalities of treatment and by the development of improved criteria for regimen design and result assessment (8-10). As a consequence of these advances, it is now possible to induce complete tumor regression in patients with different types of neoplasia and to obtain disease-free survival lasting 10 years or longer in a notable percentage of them (11-14).

Despite this progress, major difficulties remain to be overcome before cancer therapeutics may become generally successful in curative management (15-17). This is particularly observed in the case of the common solid tumors. These difficulties may be mainly attributed to the lack of agents acting uniquely and specifically on tumors, or at least having sufficiently marked selectivity of antitumor action, and resistance phenomenon (16). Over the past two decades, new vistas have been opening up in cancer therapeutics, consequent to progress made in the understanding of the molecular biology of the cancer cell, interactions between tumor cells, host regulatory mechanisms, and mechanisms responsible for different forms of resistance (18-21). The present study presents the functional effect of Congerine (AntiGan), a mucosal galectin produced in the epidermis and esophagus of the *Conger conger,* that provides immune-chemical fortification properties through its agglutinating and opsonizing activity (22). It has been demonstrated that Congerine may reach and function in the intestinal lumen since it presents marked resistance against digestion by gastric and enteric enzymes (22,23). In humans and mice, galectin-4 is known to be expressed in the alimentary canal from the tongue to the large intestine (24), and

Correspondence to: Dr Iván Carrera, Department of Health Biotechnology, EuroEspes Biotechnology, Parroquia de Guisamo A6, 15165 Corunna, Spain
E-mail: biotecnologiasalud@ebiotec.com

probably functions intracellularly in the defense of the colonic mucosal surfaces. In the present work, different concentrations of AntiGan, a lipofishin extract obtained from *C. conger*, was used to evaluate its preventive and/or therapeutic effects on colorectal adenocarcinoma cell cultures (HL60, HS 274.T, HS 313.T, H2126, WM 115, HS 281T, Caco-2, HT-29 and SW-480) and in an animal model of colon inflammation induced by dextran sulphate sodium (DSS). In light of its anti-inflammatory effect on colonic mucosal surfaces, its anti-tumor potential on apoptotic activation processes, the easy cell/tissue isolation method, and the fact that lyophilization of this bioactive product (E-Congerine) conserves their original properties, AntiGan is a promising candidate for preclinical and clinical applications in anticancer immunotherapy.

Materials and methods

Cell lines and cell culture. All cell lines were purchased from the American Type Culture Collection (Manassas, MA, USA). Human colorectal adenocarcinoma cell line (SW-480) was maintained in Leibovitz-15 medium with L-glutamine, supplemented with 10% heat-inactivated fetal bovine serum (FBS) (both from PAA; GE Healthcare Life Sciences, Little Chalfont, UK) and sodium bicarbonate (1.5 g/l) (Gibco; Thermo Fisher Scientific, Inc., Waltham, MA, USA), and incubated at 37°C in 5% CO_2. HL-60 (promyelocytic leukemia) cell line was grown in RPMI-1640 (Gibco; Thermo Fisher Scientific, Inc.) supplemented with 10% heat-inactivated FBS, 100 IU penicillin, 100 μg/ml streptomycin and 2 mM L-glutamine. HS 274.T (breast adenocarcinoma) and HS 313.T (lymphoma) cell lines were grown in Dulbecco's modified Eagle's medium (DMEM; Gibco; Thermo Fisher Scientific, Inc.) supplemented with 10% heat-inactivated FBS, 100 IU penicillin, 100 μg/ml streptomycin and 2 mM L-glutamine. H2126 hypotriploid cell line from a metastatic site, pleural effusion adenocarcinoma, was grown in DMEM/F12 (Gibco; Thermo Fisher Scientific, Inc.) supplemented with 5% heat-inactivated FBS, 100 IU penicillin, 100 μg/ml streptomycin, G5 supplement (Gibco; Thermo Fisher Scientific, Inc.) and 2 mM L-glutamine. Caco-2 colorectal adenocarcinoma cell line was grown in Eagle's minimum essential medium (EMEM; Gibco; Thermo Fisher Scientific, Inc.) supplemented with 20% heat-inactivated FBS, 100 IU penicillin, 100 μg/ml streptomycin and 2 mM L-glutamine. HT-29 colorectal adenocarcinoma cell line was grown in McCoy's 5A modified medium (Gibco; Thermo Fisher Scientific, Inc.) supplemented with 10% heat-inactivated FBS, 100 IU penicillin, 100 μg/ml streptomycin and 2 mM L-glutamine. WM 115 (melanoma) cell line was grown in EMEM, supplemented with 10% heat-inactivated FBS, 100 IU penicillin, 100 μg/ml streptomycin and 2 mM L-glutamine. HS 281.T (breast adenocarcinoma) cell line was grown in DMEM supplemented with 10% heat-inactivated FBS, 100 IU penicillin, 100 μg/ml streptomycin and 2 mM L-glutamine. Cell stocks were maintained in liquid nitrogen.

MTT reduction assay. Cell proliferation was determined using MTT assay. Cell lines ($1x10^5$ cells/ml) were incubated in 96-well plates with different doses of AntiGan (10, 25 and 50 μl/well) at 37°C for 24 h (Ebiotec, Bergondo, Spain). A total of 10 μl MTT (10 mg/ml) was added to each well and incubated

further at 37°C for 4 h. After incubation, MTT-formazan precipitate was dissolved in 100 μl dimethyl sulfoxide and absorbance was recorded at 570 nm in an ELISA plate reader. The antiproliferative effect of AntiGan was investigated in Caco-2, HT-29 and SW-480 cells, by treating them with 10, 25 and 50 μl/ml AntiGan or culture medium. Data were presented as the percentage of cytotoxicity of treated vs. untreated cells.

DNA ladder assay. DNA ladder assay was conducted as per a standard method. This method prevents the contamination of entire genomic DNA with fragmented DNA. Briefly, following treatment with AntiGan, cells were harvested (centrifugation at 27,000 x g at 4°C for 30 min), washed twice with cold PBS and lysed for 30 min at 4°C in lysis buffer (50 mM Tris-HCl, pH 7.5, 1 mM EDTA, 0.2% Triton X-100) using zirconium beads (cat. no. 11079107zx; BioSpec, Bartlesville, USA) and an automatic cell lyser. Following centrifugation at 15,000 x g at 4°C for 20 min, the supernatants were treated with protease inhibitor cocktail (cat. no. P8465-5ML; Sigma-Aldrich; Merck KGaA, Darmstadt, Germany) and 0.5% SDS for 1 h at 37°C. DNA was extracted twice with phenol and precipitated with 150 mM NaCl and two volumes of ethanol at -20°C. DNA precipitate was washed twice with cold 70% ethanol, dissolved in TE buffer (cat. no. 93283-100ML) and treated for 1 h with RNase (cat. no. 10109134001) (both from Sigma-Aldrich; Merck KGaA) at 37°C. Finally, DNA precipitates were stained with propidium iodide at room temperature (RT) for 10 min, electrophoresed on 2% agarose gel and visualized in an automatic gel documentation system (Bio-Rad Laboratories, Inc., Hercules, CA, USA).

A cytometric bead array was performed to assess the levels of interleukin (IL)-6 (cat. no. SCU0001; 1:100), IL-10 (cat. no. I17002; 1:100), IL-17 (cat. no. SRP3080; 1:100), IL-1β (cat. no. SRP6169; 1:100), interferon (IFN)-γ (cat. no. I17001; 1:100) and tumor necrosis factor (TNF)-α (cat. no. T6674; 1:100) in the samples (all from Sigma-Aldrich; Merck KGaA). Each capture bead had a distinct fluorescein isothiocyanate (FITC) conjugate and was coated with a capture antibody specific for each soluble protein. The detection reagent was a mixture of phycoerythrin (PE)-conjugated antibodies (cat. no. MABF925; 1:200; Sigma-Aldrich; Merck KGaA), which provided a fluorescent signal in proportion to the amount of bound analytes. When the capture and detection beads were incubated with the samples and controls (beads without conjugated antibodies), sandwich complexes (capture bead + analyte + detection reagent) were formed. These complexes were subsequently measured using flow cytometry to identify particles with fluorescence characteristics of both the bead and the detector.

The bead population was resolved in two fluorescence channels of a FACStar flow cytometer (Becton Dickinson; BD Biosciences, Franklin Lakes, NJ, USA) equipped with a 5 W argon ion laser emitting 488 nm at 0.2 W. Green fluorescence (FITC) was collected through a 530/30 nm filter and red fluorescence (PE) through a 585/42 nm filter. Beads with different positions were combined in the assay to create a six-plex assay. The intensity of PE fluorescence of each sandwich complex revealed the concentration of each cytokine. Data were collected in four-parameters with linear amplification for forward light scatter and logarithmic amplification for side light scatter, green and red fluorescence. Data

Table I. Oligonucleotides used in reverse transcription-polymerase chain reaction.

Gene	Direction	Sequence (5'-3')
p53	Sense	AAAACTTACCAAGGCAACTA
	Antisense	TGAAATATTCTCCATCGAGT
p21	Sense	CATGTCCGATCCTGGTGATG
	Antisense	AGTGCAAGACAGCGACAAGG
Bcl-2	Sense	TGCACCTGACGCCCTTCAC
	Antisense	AGACAGCCAGGAGAAATCAAACAG
Bcl-2-associated X protein	Sense	ACCAAGAAGCTGAGCGAGTGTC
	Antisense	ACAAAGATGGTCACGGTCTGCC

Bcl-2, B-cell lymphoma 2.

was processed using Consort 30 software (Consort BVBA, Turnhout, Belgium).

RNA isolation and reverse transcription-polymerase chain reaction (RT-PCR). Single step phenol-chloroform-isoamyl alcohol extraction was used to isolate the total cellular RNA by lysis in a guanidinium isothiocyanate buffer (cat. no. G9277-100G; Sigma-Aldrich; Merck KGaA), as previously described (25,26). RNA was converted into cDNA by reverse transcription using a Maxima Reverse Transcriptase kit (cat. no. EP0741), using reverse transcriptase M-MLV and RiboLock RNase inhibitor agents (all from Applied Biosystems; Thermo Fisher Scientific, Inc.). The primer sequences used are detailed in Table I. The concentration of cDNA was measured using a NanoDrop™ spectrophotometer (Thermo Fisher Scientific, Inc.) and the samples were preserved at -80°C. PCR was performed as follows: 40 cycles of denaturation at 95°C for 5 sec and annealing-extension at 60°C for 5 sec. 1.5% agarose gel electrophoresis was used to analyze the resulting PCR products. The primers were synthesized by Bio Basic, Inc. (Markham, ON, Canada). RT-PCR was performed using a ABI Model 7500 Sequence Detector (Applied Biosystems; Thermo Fisher Scientific, Inc.) with a SYBR-Green Real-Time PCR kit (Takara Bio, Inc., Otsu, Japan). Specific primers and their sequences are indicated in Table I. The molecular mechanisms responsible for the AntiGan activity in the cell lines used were tested by the gene expression of the following apoptotic-related genes: p53, p21, Bcl-2-associated X protein (Bax) and Bcl-2.

Animals. A total of 56 specific pathogen-free Swiss CD1 female mice (7 weeks old and 20-25 g; Santiago de Compostela's University Animal Breeding Core, Santiago de Compostela, Spain) were maintained (2 or 3 mice/cage) in isolator plastic cages with shavings under standard laboratory conditions (sterilizable diet; 50% humidity; 23-24°C temperature; and 12-h light/dark cycle). All mice were quarantined 3 weeks after arrival and then randomized by body weight into experimental and control groups. All mice were permitted free access to a commercial diet and treatment or normal drinking tap water in individual bottles. All procedures conformed to the guidelines established by the European Communities Council Directive of 24 November 1986 (86/609/EEC) and by the Spanish Royal Decree 1201/2005 for animal experimentation, and were approved by the Ethical Committee of EuroEspes Biotechnology (Coruna, Spain; EE-12/223).

Study design. The present experimental study was designed to induce colitis-associated dysplasia and/or tumor hallmarks by administering DSS (Sigma-Aldrich; Merck KGaA) to mice and feeding them a diet with different AntiGan dilutions. In the present study, the calculation of sample size was performed by power analysis (software G Power; gpower.hhu.de/en.html, version 3192) (23), which takes into account the effect size (difference between the mean of two groups), standard deviation (variability within the sample), type 1 error [significance level of 5% (P=0.05)], power of the study (probability of finding an effect, kept at 80%), direction of effect (two-tailed test), statistical tests (analysis of variance) and expected attrition (mortality of animals).

Experimental mice were separated into two control groups (D and E, n=10/group) and three treatment groups (A-C, n=12/group). AntiGan extract (E-Congerine 10423®) was integrated in the diet as pellet biscuits and elaborated in our laboratory by adding different % of powder treatment ingredients (AntiGan) using diet wheat as the main flour, adding 10% (w/w) Milli Q-purified water for pelleting and then drying the pellets at 34°C overnight. In the first 2 weeks, diet containing different AntiGan concentrations (2.5% in group A, 5% in group B, 10% in group C and 5% in group D) was administered to mice in groups A, B, C and D. In the third week, tap water containing 20 g/l (2%) synthetic DSS (mol mass, 5,000; D4911) was administered to mice in groups A, B, C and E. Control groups D and E were treated only with AntiGan or DSS, respectively. At the end of the experiment (sixth week), mice were sacrificed (15 weeks of age) and different colorectal segments and blood samples were collected for specific immunohistochemistry and staining analysis. The overall health of the mice before and after treatment was assessed and normal parameters were observed.

Tissue preparation. Mice were deeply anesthetized by inhalation of diethyl ether (cat. no. 100921; Sigma-Aldrich; Merck KGaA) and blood samples were extracted. The location, storage and use of diethyl ether was approved by the Ethical Committee of EuroEspes Biotechnology (EE-12/223), Bureau Veritas Certification (ISO 9001:2008), the European Quality

Assurance in Lab (UNE 166002:2006) and the Human Health Agency of Spain (U:75/2013). Subsequently, mice were intracardially perfused with saline buffer and then fixed by 4% paraformaldehyde (30 min at RT) in 0.1 M phosphate buffer (pH 7.4). Euthanasia was performed under anesthesia by exsanguination and cervical dislocation. Confirmation of euthanasia was performed by decapitation. The entire colorectum (from ileocecal junction to the anal verge) was removed, measured, examined macroscopically (Olympus BX50; magnification, x4), washed with saline buffer and immediately fixed by immersion in the same fixative for 48 h at RT. Part of the colon was divided into three equal segments (proximal, middle and distal), portions were determined under a dissecting stereo light microscope at x20 magnification (Leica M125; Leica Microsystems, Inc., Buffalo Grove, IL, USA). Intestine portions were cryoprotected with 30% sucrose in 0.1 M phosphate buffer, embedded in OCT compound (Tissue Tek; Sakura Finetek USA, Inc., Torrance, CA, USA), and frozen with liquid nitrogen-cooled isopentane. Parallel series of transverse sections (14-16 μm) were obtained on a cryostat (Starlet 2212; Bright Instruments, Ltd., Luton, UK) and mounted on Superfrost Plus (cat. no. 4951PLUS4; Menzel-Gläser®; Thermo Fisher Scientific, Inc.) slides.

Histological staining and immunohistochemistry. Prior to staining sections were fixed with 4% paraformaldehyde (Sigma-Aldrich; Merck KGaA) in a phosphate buffer for 48-72 h at RT. Routine histological examination was performed on 14-μm-thick hematoxylin and eosin (H&E)-stained sections (hematoxylin 60% at RT for 5 min and eosine 50% at RT for 1 min; MEDITE GmbH, Burgdorf, Germany) where different morphological alterations that occured during colorectal carcinogenesis (such as crypt abscess, mucosal dysplasia, adenomas and adenocarcinomas) (8), were identified by light microscopy (magnification, x20) and diagnosed according to a previously published study (27). To detect the expression of colorectal histopathological markers, including β-catenin, Bcl-2 and cyclooxygenase (Cox)-2, immunohistochemical techniques were used. The sections (FSC 22 frozen section media; Leica Microsystems, Ltd., Milton Keynes, UK) of 14 μm were pretreated with H_2O_2 to eliminate endogenous peroxidase, rinsed twice for 10 min each in PBS at pH 7.4, and then treated with nonspecific binding blocking solution [0.1 M PBS containing 0.2% Tween-20 and 15% normal goat serum (Dako; Agilent Technologies, Inc., Santa Clara, CA, USA)] for 1 h at RT. Following this, the sections were incubated with primary rabbit polyclonal antibodies that were affinity-purified from rabbit antiserum by affinity-chromatography using mouse epitope-specific immunogen, including anti-β-catenin, anti-Bcl-2 and anti-Cox-2 (cat. nos. BS3603, BS3736 and BS1017, respectively; dilution, 1:200; Bioworld Technology, Inc., St. Louis Park, MN, USA) overnight at RT. The sections were then washed in PBS (two 10-min rinses), incubated with goat anti-rabbit immunoglobulin G serum biotinylated (cat. no. E-0432; dilution, 1:100; Dako; Agilent Technologies, Inc.) for 1 h at RT, washed with PBS (two 10-min rinses), treated with a Vectastain ABC kit (Vector Laboratories, Inc., Burlingame, CA, USA) for 1 h at RT, and finally washed again in PBS (two 10-min rinses). As a negative control, omission of the primary, secondary or tertiary antibodies was used and

no immunostaining was observed. At the last step, the immunoreaction was developed with 0.005% diaminobenzidine (Sigma-Aldrich-Aldrich; Merck KGaA) and 0.003% H_2O_2. All dilutions were made in PBS containing 0.2% Tween-20, and incubations were made in a humid chamber at RT. Finally, the sections were dehydrated, mounted and cover-slipped.

Antibody characterization and specificity. According to the technical information supplied by the manufacturer (Bioworld Technology, Inc.), the primary antibodies used were raised against denatured mouse epitopes from rabbit antiserum and they were affinity-purified by chromatography using epitope-specific immunogen with purity >95% (by SDS-PAGE). Its specificity has been assessed by western blotting; it recognizes a single protein band of 86-90 kD (β-catenin), 26-28 kD (Bcl-2) and 74-76 kD (Cox-2). Additionally, antibodies have wide species cross-reactivity and were used for demonstrating their expression in mice, rats and humans.

In the present study, lesions were classified as positive for β-catenin/Bcl-2/Cox-2 if cytoplasmic/nuclear staining was detected. Two different observers individually and independently evaluated the experimental group slides in a double-blind manner and achieved a high level of concordance.

Imaging. The sections were photographed with an Olympus microscope (BX50) equipped with a color digital camera (DP10; magnification, x20; both from Olympus Corporation, Tokyo, Japan). The photographs were converted to grayscale and adjusted for brightness and contrast with Corel Draw and the image size was adjusted with Corel Photo Paint version 11 (Corel Corporation, Ottawa, ON, Canada).

Statistical analysis. The statistical parameters of the results obtained were performed using SPSS v.11.0 (SPSS, Inc., Chicago, IL, USA). Differences between treated groups were compared with Kruskal-Wallis test followed by Mann-Whitney U test for nonparametric data, while normally distributed data was tested using the one-way analysis of variance. Bonferroni's correction was used to avoid false positives while Games-Howell was used to compare combinations of treatment groups. Data was presented as the mean ± standard error of the mean. $P<0.05$ was considered to indicate a statistically significant difference.

Results

AntiGan treatment inhibits growth in tumor cell lines. In order to analyze the possible antineoplastic effect of AntiGan in different tumor cell lines, its effect on cell growth was assessed by MTT assay, measuring the live cell metabolism rates based on the enzyme activity levels of mitochondrial dehydrogenase. Results demonstrated that AntiGan induced cell growth inhibition in a dose-dependent manner in the majority of cell lines used (Fig. 1). The cytotoxicity detected was not restricted to a specific tumor cell line, as five different cell lines were sensitive to the effects of AntiGan. The highest level of growth inhibition was observed in Caco-2 (66, 75.8 and 88.1% growth inhibition for 10, 25 and 50 μl/ml AntiGan, respectively), HT-29 (56, 73 and 86% growth inhibition for 10, 25 and 50 μl/ml AntiGan, respectively) and SW-480 (38.5, 61.6
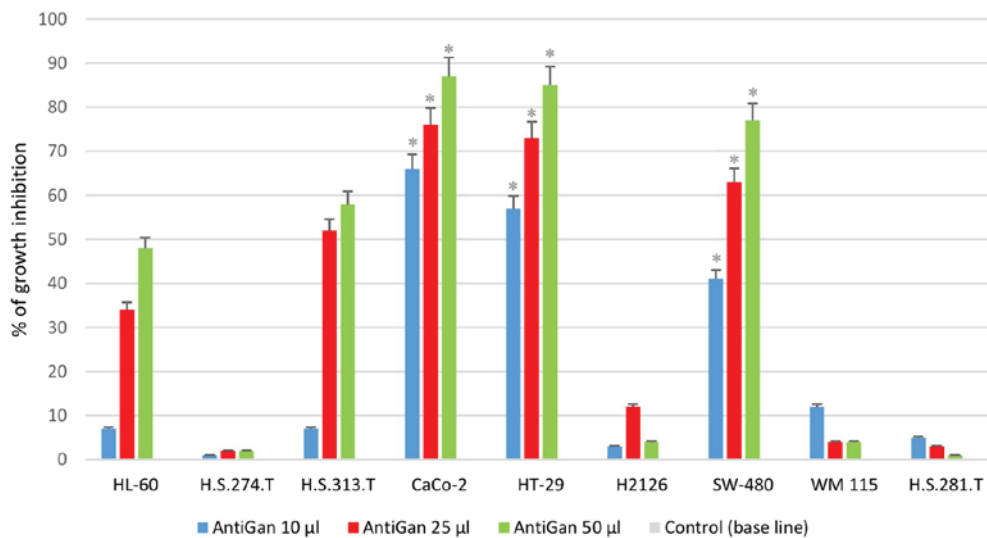
Figure 1. Growth inhibition of HL-60, HS 274.T, HS 313.T, H2126, WM 115, HS 281.T, Caco-2, HT-29 and SW-480 human tumor cell lines. Cell lines were plated on 96-well plates and exposed to three doses of AntiGan (10, 25 and 50 μl/ml). The growth inhibition is indicated as a percentage of the total cells compared with the control (culture medium). *P<0.05 vs. the control. The control group is the base line of the graph. All values are mean of triplicate cultures in five independent experiments.

and 78.6% growth inhibition for 10, 25 and 50 μl/ml AntiGan, respectively) cells; while HL-60 (5.8, 33.5 and 47.1% growth inhibition for 10, 25 and 50 μl/ml AntiGan, respectively) and HS 313.T (5.3, 50.3 and 59.6% growth inhibition for 10, 25 and 50 μl/ml AntiGan, respectively) cells demonstrated a slight, cytotoxic effect with respect to untreated cells. At the lowest concentration of AntiGan (10 μl/ml) a significant difference between controls (untreated) and treated cells was observed in Caco-2, HT-29 and SW480 cell lines. No significant cytotoxic effects were observed in the HS 274.T, H2126, WM 115 and HS281.T tumor cell lines.

In order to address if the antiproliferative effect of AntiGan was reversible, Caco-2, HT-29 and SW-480 cells were treated with 25 μl/ml AntiGan or culture medium. After 48 h of incubation with AntiGan, the cell density was reduced by >50% in all cell lines. Once AntiGan was removed from the cell culture, the cell density showed a small decrease, while in the absence of treatment, as expected, cell density increased with time (Fig. 2). These data indicate that the AntiGan effect was not reversible.

AntiGan induces apoptosis in tumor cell lines. In order to analyze if there are any cytotoxic effects of AntiGan, HL-60, HS 274.T, HS 313.T, H2126, Caco-2, WM 115, HT-29, SW-480 and HS 281.T human tumor cell lines were treated with 25 μl/ml AntiGan. Microscopic analysis of SW-480 cells revealed that numerous cells exhibited condensation (arrows) and cleavage of their nuclei, characteristic of an apoptotic process (Fig. 3A). These apoptotic hallmarks were not observed in control (untreated) cells (Fig. 3B). The results obtained, expressed as absorbances (570 nm), indicated that treatment with AntiGan induced apoptosis in the HL-60 cell line. DNA prepared from HL-60, HS 313.T, Caco-2, SW-480 and HT-29 cell lines treated with AntiGan demonstrated oligonucleosomal ladder fragmentation on agarose gel electrophoresis (data not shown). No signs of apoptosis were observed in HS 274.T, H2126, WM 115 and HS 281.T cells (data not shown).
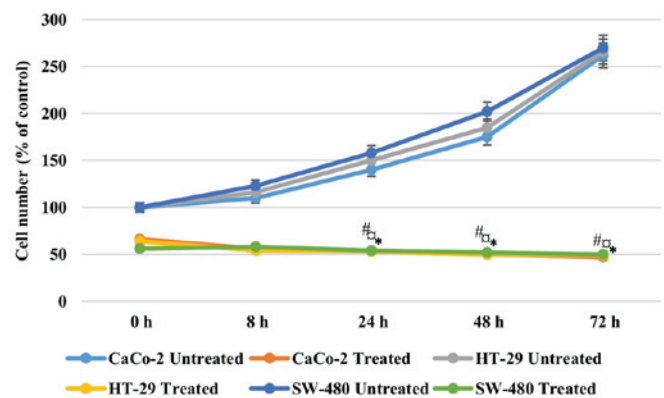

Figure 2. Anti-proliferative effects of AntiGan in Caco-2, HT-29 and SW-480 cells. Cell lines were treated for 48 h with 25 μl/ml AntiGan (treated) or complete medium (untreated). Results are expressed relative to the control (48 h incubation with medium). *P<0.05 vs. CaCo-2 untreated cells; °P<0.05 vs. HT-29 untreated cells; #P<0.05 vs. SW-480 untreated cells. The mean shown was calculated from three independent experiments performed in triplicate.

AntiGan treatment downregulates Bcl-2 gene expression. In order to study the molecular mechanisms of AntiGan that induced apoptosis in HL-60, HS 313.T, Caco-2, HT-29 and SW-480 cell lines, the gene expression patterns of some apoptotic-associated genes, including p53, p21, Bax and Bcl-2, were analyzed following treatment with AntiGan (10, 25 and 50 μl/ml) by RT-PCR. AntiGan treatment (10 μl/ml) triggered downregulation of Bcl-2 gene expression in all cell lines, with no significant effect on the expression levels of the other genes, resulting in the relative increase of Bax/Bcl-2 ratio (Fig. 4). AntiGan treatment at 25 and 50 μl/ml did not have a significant effect on the expression level of the genes that were investigated (data not shown).

Pathological and inflammatory findings. Experimental mice treated with 2% DSS and lower or absent concentrations of
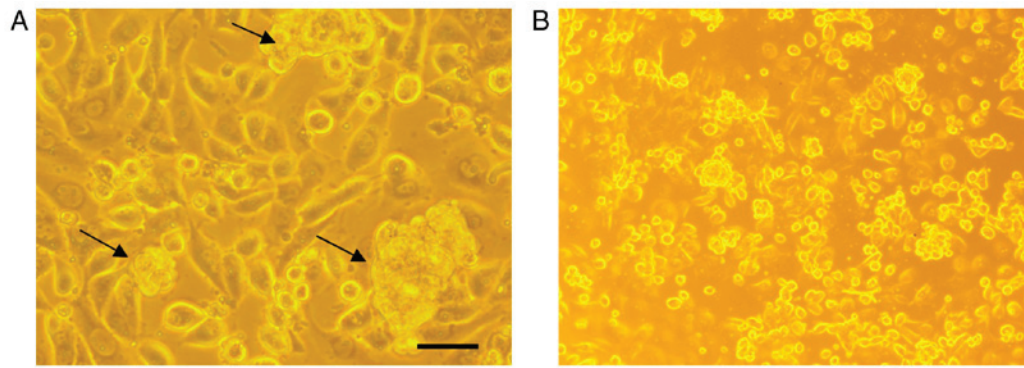
Figure 3. Morphological examination of AntiGan-treated SW-480 cells. SW-480 cells were cultured in the (A) presence or (B) absence of 25 µl/ml AntiGan for 24 h. The morphological organization of the cells was examined by light microscopy. The black arrows indicate nuclear condensation. Magnification, x40.
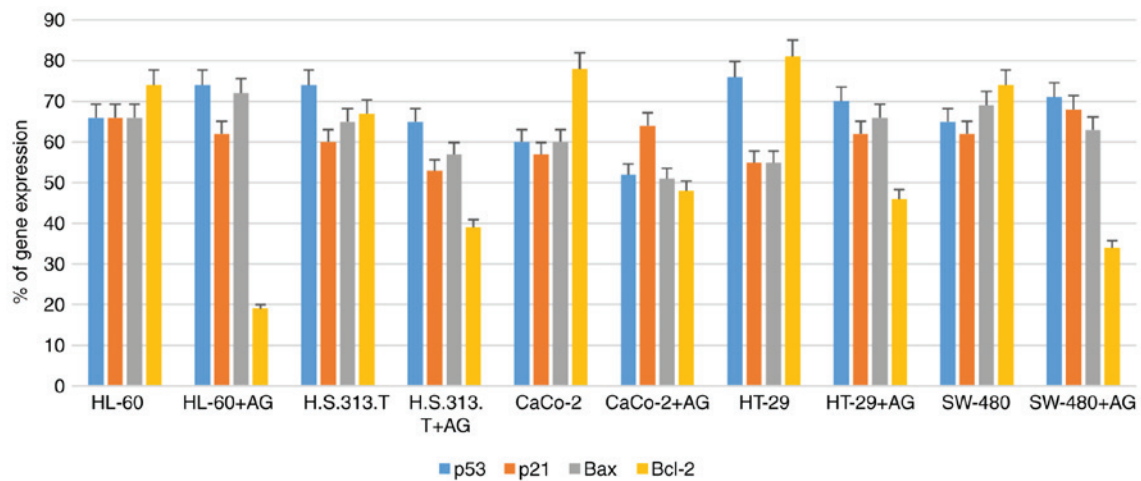

Figure 4. Detection and quantification of apoptotic-related gene expression in tumor cell lines treated with AG. The downregulation of Bcl-2 gene expression was induced by AG treatment, while other genes were not significantly affected, leading to the relative increase of Bax/Bcl-2 ratio. AG, AntiGan; Bcl-2, B-cell lymphoma 2; Bax, B-cell lymphoma 2-associated X protein.

AntiGan (groups A and E) exhibited bloody stools from the third week of experimentation, while no such inflammatory effects were noticed in any other group. A macroscopic evaluation (data not shown) recognized some gross inflammatory polypoids in groups E (6/6; 100%) and A (5/6; 83.3%), with the majority of them located in the middle and distal portions of the colorectal segment, while only few of them were identified in group D (1/6; 16.6%). Notably, no mice in group C (DSS/10% AntiGan) demonstrated these ulcerative hallmarks, similar to that observed in the control mice (group D; 5% AntiGan). This macroscopic evaluation profile was corroborated by microscopic analysis of the histological colorectal morphology, with special identification of inflammatory hallmarks on the colonic mucosa and submucosa, mainly represented by dysplastic epithelium and ulcerative alterations. The histological observation of hematoxylin and eosin-stained sections (Fig. 5) revealed some ulcers that represent a severe inflammation hallmark within the submucosa and mucosal areas. Additionally, there were also some moderate crypt hyperplasia (epithelium with abnormal thickness), and epithelial dysplasia, which is the alteration of the normal differentiation process of epithelial cells that may progress to invasive colorectal carcinoma (17). However, the presence of these inflammatory alterations and their severity differed among the experimental

treatment groups. Mice in group E, only treated with DSS, demonstrated high severity levels of these colorectal inflammatory hallmarks, which was in contrast to the moderate and mild lesion levels observed in mice treated with increased concentrations of AntiGan (groups A and B, respectively). These characteristic colitic alterations were mild or absent in the colorectal samples of mice treated with high concentrations of AntiGan (group C). Mice treated only with AntiGan (control group D; 5% AntiGan), demonstrated no adverse effects or histological alterations at microscopic examination (Fig. 5).

Immunohistochemistry of β-catenin, Bcl-2 and Cox-2. Immunohistological markers with high specific affinity against colorectal cell epitopes demonstrated notable expression levels of β-catenin (cellular adhesion regulator), Bcl-2 (apoptotic regulator) and Cox-2 in colorectal lesions in mice. By using β-catenin polyclonal antibody, the endogenous expression levels of β-catenin protein within the cytoplasm of affected colorectal cell layers were observed. As expected, high immunoreactive expression levels of β-catenin were detected in the proximal and middle colon segments (Fig. 5T) in mice treated with DSS, similar to the moderate immunoreactivity patterns observed in the colorectal segments (Fig. 5D and H) of mice
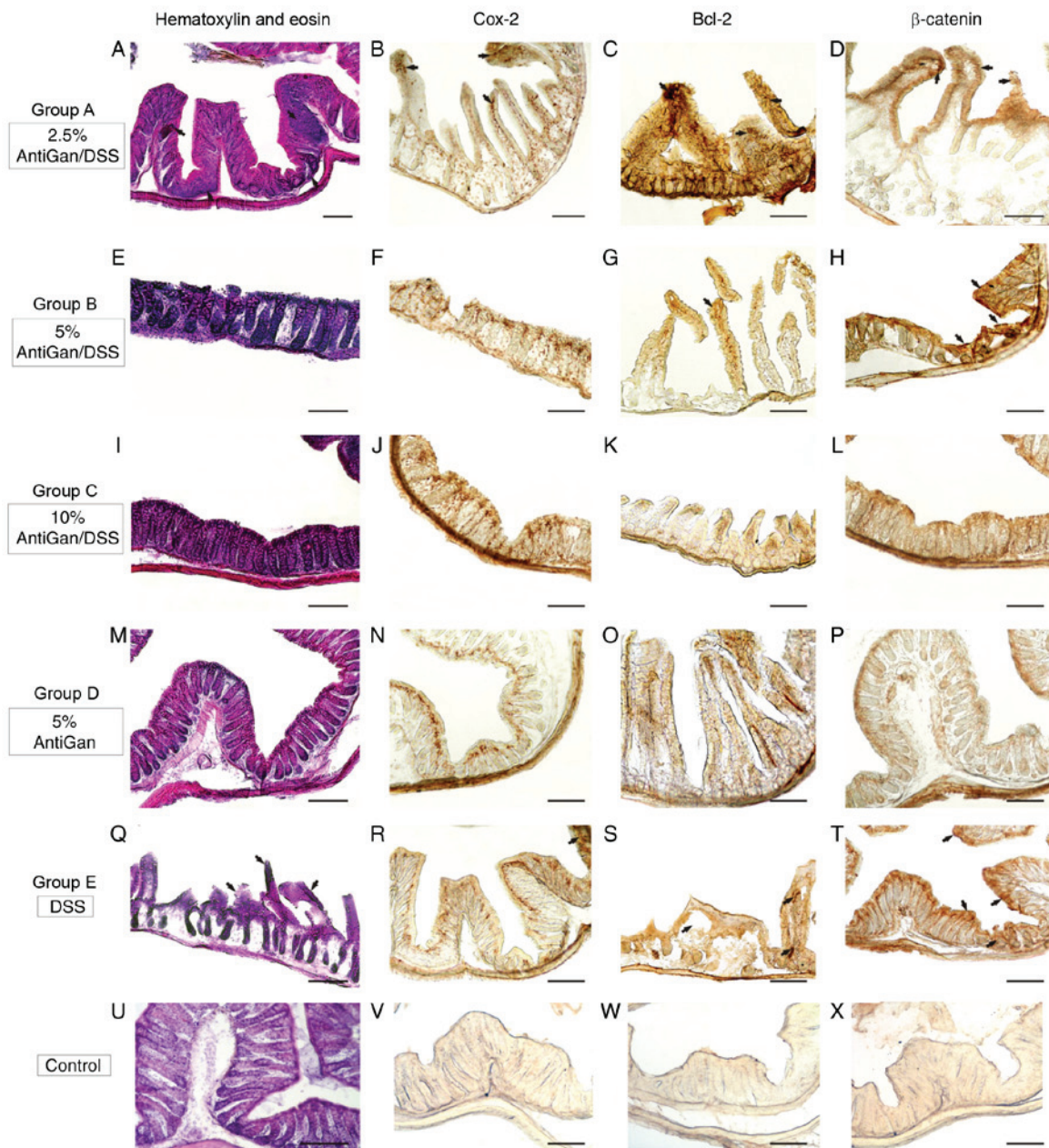
Figure 5. Photomicrographs of different portions of colon from experimental mice showing histopathological lesions identified by hematoxylin and eosin staining, and immunohistochemical detection. (A-H) Details of transverse sections at the middle and distal colorectal levels of mice in groups A and B (arrows), demonstrating high-moderate immunoreactivity to β-catenin, Bcl-2, and Cox-2. (I-L) Colorectal sections of mice in group C demonstrated a normal colonic epithelial organization with well-differentiated cryptal cells. (M-P) Details of colorectal sections of mice in group D, to highlight the strong immunoreactive staining of the cell markers. (Q-T) A high density of immunoreactive cells (arrows) were observed in mice in group E and these were gathered at specific pathological lesions, demonstrating a severe-grade of dysplasia. (U-X) Negative control sections. Scale bar, 100 μm. DSS, dextran sulphate sodium; Bcl-2, B-cell lymphoma 2; Cox-2, cyclooxygenase-2.

treated with low concentrations of AntiGan (DSS/2.5-5% AntiGan). These β-catenin immunoreactive cells were mainly observed in the internal cryptal layers, being characterized histologically as dysplastic cryptal cells and adenocarcinoma cells (Fig. 5H and T). However, cryptal cells of the colorectal segments of mice treated with high AntiGan concentrations (group C) demonstrated a weak or absent β-catenin immunoreactivity (Fig. 5L), similar to the control (Fig. 5X), as compared with the β-catenin cellular basal expression of group D (Fig. 5P). A similar immunostaining pattern was obtained when detecting reactivity levels of Bcl-2, an anti-apoptotic oncoprotein, in the colorectal portions of groups A (Fig. 5C),

B (Fig. 5G) and E (Fig. 5S). Bcl-2 immunoreactivity was specifically intense in the adenocarcinoma and cryptal cells of colorectal portions of mice treated with DSS. Intense Bcl-2 staining patterns were mild or completely absent in colorectal section of mice groups C, D and control, respectively (Fig. 5K, O and W, respectively). A strong staining pattern of Cox-2 in immunoreactive cryptal cells was observed in the colorectal dysplastic epithelium of mice treated with DSS (Fig. 5R) and lower concentrations of AntiGan (Fig. 5B), being particularly intense in group E. Immunoreactive staining signal of Cox-2 was mild or absent in colorectal portions of mice from groups B, C, D and control (Fig. 5F, J, N and V, respectively).

Table II. Production of pro-inflammatory cytokines in mice with dextran sulphate sodium-induced colitis treated with AntiGan.

| Treatment | Pro-inflammatory cytokines, pg/ml | | | | | |
	IL-1β	IL-6	IL-10	IL-17	Interferon-γ	Tumor necrosis factor-α
Negative control	8.5	11.7	10.6	12.3	13.2	11.3
AntiGan						
2.5 μl/ml	9.2	12.5	11.5	12.6	12.6	16.1
5 μl/ml	10.3	11.2	13.5	12.6	28.7	11.1
10 μl/ml	17.1	13.6	12.8	11.3	71.7[a]	12.6
Positive control	55.7	17.7	19.3	12.6	99.3	77.5

IL, interleukin. [a]$P<0.005$ vs. negative control for interferon-γ.

DSS induces the production of inflammatory cytokines. In order to address the potential mechanisms that may trigger colitis generated by continuous treatment with DSS and the possible beneficial effect of AntiGan in the diet, a proinflammatory cytokine analysis was performed by cytokine zirconium beads arrays. DSS treatment in mice significantly increased the production of the proinflammatory cytokine interferon (IFN)-γ compared with the levels in the negative control group. There were no significant changes in the production levels of other cytokines, including interleukin (IL)-1β, tumor necrosis factor (TNF)-α, IL-6, IL-10 and IL-17, in both treated and untreated mice (Table II).

Discussion

In order to understand and treat human diseases, natural components have been discovered and used for thousands of years by all civilizations and cultures in the world. Previous studies estimated that ~25% of the drugs prescribed worldwide are derived from plant excipients and 60% of anti-tumor/anti-infectious drugs already on the market or under clinical trial are of natural origin (27-34). Thus, plant extracts derived from Taxol, curcumin, phenolic acids and flavonoids are reported to inhibit tumor cell growth (27-34).

It is known that there are at least 120 chemical substances that are useful as antineoplastic drugs, such as Paclitaxel (Taxol, genus *Taxus*), and are isolated from plants; although research data regarding the role of natural compounds in the treatment of different types of tumors is required (27-34). An increasing number of epidemiological studies assessing dietary intake of natural compounds, based on biological and healthy effects, have provided data supporting an inverse correlation between reduced risk and bioactive effect of the tested compounds (27-34). Although AntiGan has demonstrated significant antineoplastic activities, *in vitro* and *in vivo,* against different tumor cell lines, the molecular mechanism underlying this effect has not been sufficiently studied. In the present investigation, AntiGan demonstrated selective cytotoxicity *in vitro* for different human tumor cell lines (pro-myelocitic and colon cancer cell lines) when compared to untreated cells. The unusual ability that AntiGan has demonstrated to effectively kill several types of tumor cells without significant cytotoxicity to normal control cells suggests that AntiGan

may be a potential chemotherapeutic agent. The present data indicated that AntiGan induces apoptosis in specific cell lines, in a dose-dependent manner, probably generated by three main cellular metabolic events, including the alteration of the mitochondrial transmembrane potential, and the activation of caspase-3 and caspase-8 pathways (35-43). The results obtained in the present study indicate that AntiGan inhibits the process of tumor cell proliferation by inducing cell death through the activation of cytotoxic mechanisms.

Apoptosis is a genetically- and epigenetically-directed process of cell self-destruction that is marked by the fragmentation of nuclear DNA, resulting in programmed cell death; however, when halted, it may lead to uncontrolled cell growth and tumor formation (32-35). Apoptosis may be triggered in a cell through either the extrinsic or the intrinsic pathway: i) Positive stimulation of the transmembrane death receptor (Fas receptor and caspases); and ii) active release of intracellular apoptotic signal factors (32-39). Positive stimulation involves ligands related to TNF, while the induction of apoptosis by the release of signal factors involves the mitochondria (35). It is known that most types of tumor cell mechanisms are triggered by the activity of dysfunctional apoptotic enzymes and by the balance disturbance between apoptotic and proliferation processes (36). Two types of apoptotic-related genes (Bcl-2 family) regulate these intracellular mechanisms: Apoptotic repressor (Bcl-2) and apoptotic promoter (Bax). Research has suggested that encoded proteins combined with Bcl-2 may resist the action of repressing apoptosis, but also trigger a positive regulatory action based on high Bcl-2/Bax ratios (37). All tumor cell lines used in the present study have been induced by numerous chemical agents (AT101, Brassinin, Erastin and MI-AF) to induce apoptosis through different pathways, including p53-dependent or Bcl-2 family-related pathways.

In order to address the molecular mechanism of apoptosis mediated by different concentrations of AntiGan, the present study investigated the expression of apoptotic-related genes, including p53, p21, Bax and the Bcl-2 family by RT-PCR. The data obtained suggested that apoptosis occurred in HL-60, HS 313T, Caco-2, HT-29 and SW-480 cell lines treated with 10 μl/ml of AntiGan, where a dose-dependent downregulation of Bcl-2 gene expression was observed. The expression levels of Bcl-2 in the other cell lines were not markedly altered. These results also indicated that the relative increase of apoptotic

EXPERIMENTAL AND THERAPEUTIC MEDICINE 15: 2547-2556, 2018

2555

Bax/Bcl-2 ratio was associated with AntiGan-induced apoptosis in different human cell lines. It is possible that AntiGan, through an appropriate signal, induces a conformational change in Bax that modifies the mitochondrial membrane, inducing the release of cytochrome c from the mitochondrial membrane into the cytosol. Taken together, the results of the *in vitro* studies demonstrated that AntiGan exhibited an apoptotic-inducing effect in different human tumor cell lines. Although further research is required to elucidate the specific mechanisms by which AntiGan induces apoptosis in some tumor cell lines, the present results indicate that AntiGan may be a useful chemotherapeutic compound for patients with different types of tumors.

In order to address the effect of AntiGan on colonic inflammation *in vivo*, mice were exposed to DSS in drinking water to induce ulcerative colitis. After 6 weeks of experimental treatment, the analytical results performed in this model of colon carcinogenesis demonstrated that AntiGan promoted a slight reduction of colorectal histopathological hallmarks at lower doses (2.5% AntiGan) and a moderate to almost complete reduction at higher doses (5-10% AntiGan). In addition, histological samples of different colon segments indicated that AntiGan has no adverse effects on the morphological organization of the structured colonic cell types, as demonstrated when analyzing mice treated with AntiGan alone in the diet. Therefore, these promising results indicate that AntiGan may be an important chemopreventive agent against colon carcinogenesis.

In the present experimental study, colorectal lesions were induced by a specific chemo-ulcerative agent to evaluate the effects of a possible antitumor agent on chronic ulcerative colitis in mice. The continuous administration of DSS as a chemical inductor agent of ulcerative lesions in murine models has been extensively reported (27,38-43), and such studies are crucial to improve our knowledge of the complex interactions between the social environment, genetics of each population, and epithelial barrier dysfunction in human-related inflammatory bowel disease (IBD) (44-46). In the present study, as reported in the experimental results of the murine model of acute colon injury, the administration of DSS in drinking water resulted in colonic epithelial damage accompanied by a strong inflammatory response. The results obtained by analyzing the dose-response effect of AntiGan throughout the different experimental groups indicated that the optimal dose-response was the 10% AntiGan concentration in diet, where no histological alterations or notable lesions were detected. The present study also indicated a clear association between AntiGan dose and the ulcerative effects observed in the colon, where progressive severity on colorectal lesions was observed with lower doses of AntiGan. These results reinforce the assumption that AntiGan may act as a chemopreventive agent against carcinogenesis without interfering with the normal epithelial histoarchitecture of the colon (45,46).

In the present study, a significant increase in the expression level of IFN-γ was observed in DSS-induced ulcerative colitis. When translated into humans, it is clear that one of most significant clues to understand ulcerative colitis (UC) and associated pathologies is the alteration of various cytokines that have been extensively reported in patients with IBD (47). Another parameter of active IBD is the imbalance between regulatory T cells (Th3) and effector T cells (Th1 and Th2). It is known that Crohn's disease is closely related to the Th1 T-cell cytokine profile (IFN-γ, TNF-α and IL-12), while UC is related to a modified Th2-type response cytokine profile (IL-10 and IL-15) (38). Recent findings have indicated that the IL-23/IL-17 axis may be part of the effector T cell immunological response, which is involved in IBD development (45). These conclusions suggest that increased levels of IL-23 and IL-17 expression are characteristic biomarkers of patients with active IBD.

Further research is required before the specific mechanism of action of AntiGan may be fully elucidated for the prevention and treatment of colitis. The present study demonstrated that AntiGan displays a preventive effect against premalignant tissue damage in a murine model of colitis, inhibiting the development of colorectal ulcers and, consequently, progressive tumors. AntiGan has been indicated to be a promising agent for chemoprevention of colon carcinogenesis.

Acknowledgements

References

 1. Eckhardt S: Recent progress in the development of anticancer agents. Curr Med Chem Anticancer Agents 2: 419-439, 2002.
 2. Medina D, Sivaraman L, Hilsenbeck SG, Conneely O, Ginger M, Rosen J and Omalle BW: Mechanisms of hormonal prevention of breast cancer. Ann N Y Acad Sci 952: 23-35, 2001.
 3. Muller E, Gasparutto D and Cadet J: Chemical synthesis and biochemical properties of oligonucleotides that contain the (5'S,5S,6S)-5',6-cyclo-5-hydroxy-5,6-dihydro-2'-deoxyuridine DNA lesion. Chembiochem 3: 534-542, 2002.
 4. Song Y, Wu F and Wu J: Targeting histone methylation for cancer therapy: Enzymes, inhibitors, biological activity and perspectives. J Hematol Oncol 9: 49, 2016.
 5. Gregory RK, Hill ME, Moore J, A'Hern RP, Johnston SR, Blake P, Shephard J, Barton D and Gore ME: Combining platinum, paclitaxel and anthracycline in patients with advanced gynaecological malignancy. Eur J Cancer 36: 503-507, 2000.
 6. Spielmann M, Llombart A, Zelek L, Sverdlin R, Rixe O and Le Cesne A: Docetaxel-cisplatin combination (DC) chemotherapy in patients with anthracycline-resistant advanced breast cancer. Ann Oncol 10: 1457-1460, 1999.
 7. Jelliffe AM: Vinblastine in the treatment of Hodgkin's disease. Br J Cancer 23: 44-48, 1969.
 8. Lech G, Słotwiński R, Słodkowski M and Krasnodębski IW: Colorectal cancer tumour markers and biomarkers: Recent therapeutic advances. World J Gastroenterol 22: 1745-1755, 2016.
 9. Spiegelberg D, Stenberg J, Haylock AK and Nestor M: A real-time in vitro assay as a potential predictor of in vivo tumor imaging properties. Nucl Med Biol 43: 12-18, 2016.
10. Wolff AC: Systemic therapy. Curr Opin Oncol 11: 468-474, 1999.
11. Gobbo OL, Sjaastad K, Radomski MW, Volkov Y and Prina-Mello A: Magnetic nanoparticles in cancer theranostics. Theranostics 5: 1249-1263, 2015.
12. de Campos-Lobato LF, Geisler DP, da Luz Moreira A, Stocchi L, Dietz D and Kalady MF: Neoadjuvant therapy for rectal cancer: The impact of longer interval between chemoradiation and surgery. J Gastrointest Surg 15: 444-450, 2011.
13. Bechis SK, Carroll PR and Cooperberg MR: Impact of age at diagnosis on prostate cancer treatment and survival. J Clin Oncol 29: 235-241, 2011.
14. Krug U, Röllig C, Koschmieder A, Heinecke A, Sauerland MC, Schaich M, Thiede C, Kramer M, Braess J, Spiekermann K, et al: Complete remission and early death after intensive chemotherapy in patients aged 60 years or older with acute myeloid leukaemia: A web-based application for prediction of outcomes. Lancet 376: 2000-2008, 2010.

15. Berz D and Wanebo H: Targeting the growth factors and angiogenesis pathways: Small molecules in solid tumors. J Surg Oncol 103: 574-586, 2011.
16. Jeong JK, Moon MH, Seo JS, Seol JW, Lee YJ and Park SY: Sulforaphane blocks hypoxia-mediated resistance to TRAIL-induced tumor cell death. Mol Med Rep 4: 325-330, 2011.
17. Villanueva A and Llovet JM: Targeted therapies for hepatocellular carcinoma. Gastroenterology 140: 1410-1426, 2011.
18. Kline J and Gajewski TF: Clinical development of mAbs to block the PD1 pathway as an immunotherapy for cancer. Curr Opin Investig Drugs 11: 1354-1359, 2010.
19. Goldman A: Tailoring combinatorial cancer therapies to target the origins of adaptive resistance. Mol Cell Oncol 3: e1030534, 2015.
20. Brett-Morris A, Mislmani M and Welford SM: SAT1 and glioblastoma multiforme: Disarming the resistance. Mol Cell Oncol 2: e983393, 2015.
21. Bustany S, Bourgeais J, Tchakarska G, Body S, Hérault O, Gouilleux F and Sola B: Cyclin D1 unbalances the redox status controlling cell adhesion, migration, and drug resistance in myeloma cells. Oncotarget 7: 45214-45224, 2016.
22. Nakamura O, Inaga Y, Suzuki S, Tsutsui S, Muramoto K, Kamiya H and Watanabe T: Possible immune functions of congerin, a mucosal galectin, in the intestinal lumen of Japanese conger eel. Fish Shellfish Immunol 23: 683-692, 2007.
23. Faul F, Erdfelder E, Lang AG and Buchner A: G*Power 3: A flexible statistical power analysis program for the social, behavioral, and biomedical sciences. Behav Res Methods 39: 175-191, 2007.
24. Huflejt ME and Leffler H: Galectin-4 in normal tissues and cancer. Glycoconj J 20: 247-255, 2004.
25. Yalon M, Tuval-Kochen L, Castel D, Moshe I, Mazal I, Cohen O, Avivi C, Rosenblatt K, Aviel-Ronen S, Schiby G, *et al*: Overcoming resistance of cancer cells to PARP-1 inhibitors with three different drug combinations. PLoS One 11: e0155711, 2016.
26. Perše M and Cerar A: Morphological and molecular alterations in 1,2 dimethylhydrazine and azoxymethane induced colon carcinogenesis in rats. J Biomed Biotechnol 2011: 473964, 2011.
27. Lombardi VR, Etcheverría I, Carrera I, Cacabelos R and Chacón AR: Prevention of chronic experimental colitis induced by dextran sulphate sodium (DSS) in mice treated with FR91. J Biomed Biotechnol 2012: 826178, 2012.
28. Barbuti AM and Chen ZS: Paclitaxel through the ages of anticancer therapy: Exploring its role in chemoresistance and radiation therapy. Cancers (Basel) 7: 2360-2371, 2015.
29. Shindikar A, Singh A, Nobre M and Kirolikar S: Curcumin and resveratrol as promising natural remedies with nanomedicine approach for the effective treatment of triple negative breast cancer. J Oncol 2016: 9750785, 2016.
30. Orfali GD, Duarte AC, Bonadio V, Martinez NP, de Araújo ME, Priviero FB, Carvalho PO and Priolli DG: Review of anticancer mechanisms of isoquercitin. World J Clin Oncol 7: 189-199, 2016.
31. Lall RK, Adhami VM and Mukhtar H: Dietary flavonoid fisetin for cancer prevention and treatment. Mol Nutr Food Res 60: 1396-1405, 2016.
32. Ediriweera MK, Tennekoon KH, Samarakoon SR, Thabrew I and Dilip DE Silva E: A study of the potential anticancer activity of *Mangifera zeylanica* bark: Evaluation of cytotoxic and apoptotic effects of the hexane extract and bioassay-guided fractionation to identify phytochemical constituents. Oncol Lett 11: 1335-1344, 2016.

33. Martínez-Pérez C, Ward C, Turnbull AK, Mullen P, Cook G, Meehan J, Jarman EJ, Thomson PI, Campbell CJ, McPhail D, *et al*: Antitumour activity of the novel flavonoid Oncamex in preclinical breast cancer models. Br J Cancer 114: 905-916, 2016.
34. Czyżewska U, Siemionow K, Zaręba I and Miltyk W: Proapoptotic activity of propolis and their components on human tongue squamous cell carcinoma cell line (CAL-27). PLoS One 11: e0157091, 2016.
35. Spilioti E, Jaakkola M, Tolonen T, Lipponen M, Virtanen V, Chinou I, Kassi E, Karabournioti S and Moutsatsou P: Phenolic acid composition, antiatherogenic and anticancer potential of honeys derived from various regions in Greece. PLoS One 9: e94860, 2014.
36. Giovannini C and Masella R: Role of polyphenols in cell death control. Nutr Neurosci 15: 134-149, 2012.
37. Fu J, Dang Z, Deng Y and Lu G: Regulation of c-Myc and Bcl-2 induced apoptosis of human bronchial epithelial cells by zinc oxide nanoparticles. J Biomed Nanotechnol 8: 669-675, 2012.
38. Cho JY, Chang HJ, Lee SK, Kim HJ, Hwang JK and Chun HS: Amelioration of dextran sulfate sodium-induced colitis in mice by oral administration of beta-caryophyllene, a sesquiterpene. Life Sci 80: 932-939, 2007.
39. Araki Y, Mukaisyo K, Sugihara H, Fujiyama Y and Hattori T: Increased apoptosis and decreased proliferation of colonic epithelium in dextran sulfate sodium-induced colitis in mice. Oncol Rep 24: 869-874, 2010.
40. Huang TC, Tsai SS, Liu LF, Liu YL, Liu HJ and Chuang KP: Effect of Arctium lappa L. in the dextran sulfate sodium colitis mouse model. World J Gastroenterol 16: 4193-4199, 2010.
41. Choi SY, Hur SJ, An CS, Jeon YH, Jeoung YJ, Bak JP and Lim BO: Anti-inflammatory effects of inonotus obliquus in colitis induced by dextran sodium sulfate. J Biomed Biotechnol 2010: 943516, 2010.
42. Whittem CG, Williams AD and Williams CS: Murine colitis modeling using dextran sulfate sodium (DSS). J Vis Exp 19: pii: 1652, 2010.
43. Slattery ML, Curtin KP, Edwards SL and Schaffer DM: Plant foods, fiber, and rectal cancer. Am J Clin Nutr 79: 274-281, 2004.
44. Okayasu I, Hana K, Nemoto N, Yoshida T, Saegusa M, Yokota-Nakatsuma A, Song SY and Iwata M: Vitamin A inhibits development of dextran sulfate sodium-induced colitis and colon cancer in a mouse model. Biomed Res Int 2016: 4874809, 2016.
45. Miner-Williams WM and Moughan PJ: Intestinal barrier dysfunction: Implications for chronic inflammatory conditions of the bowel. Nutr Res Rev 29: 40-59, 2016.
46. Wang JG, Wang DF, Lv BJ and Si JM: A novel mouse model for colitis-associated colon carcinogenesis induced by 1,2-dimethylhydrazine and dextran sulfate sodium. World J Gastroenterol 10: 2958-2962, 2004.
47. Liu Z, Feng BS, Yang SB, Chen X, Su J and Yang PC: Interleukin (IL)-23 suppresses IL-10 in inflammatory bowel disease. J Biol Chem 287: 3591-3597, 2012.